# DYNAMIC GAS TRANSPORT IN POROUS BIDISPERSED ALUMINA

Vladimir HEJTMANEK[1], Pavel CAPEK[2], Olga SOLCOVA[3] and Petr SCHNEIDER[4]

*Institute of Chemical Process Fundamentals, Academy of Sciences of the Czech Republic, 165 02 Prague 6-Suchdol, Czech Republic; e-mail: [1] hejtmanek@icpf.cas.cz , [2] pavel.capek@masch-bau.uni-magdeburg.de, [3] solcova@icpf.cas.cz, [4] schneider@icpf.cas.cz*

Received June 10, 1998
Accepted July 20, 1998

A spontaneous temporary rise in the pressure gradient through countercurrent binary transport of inert gases in porous bidispersed alumina was observed in diffusion cell of the Wicke–Kallenbach type. Experimental pressure responses to gas step changes were detected and fitted to a set of partial differential equations. These were based on the transport models Mean Transport Pore Model (MTPM) and Dusty Gas Model (DGM). The dynamic set transport parameters $\langle r \rangle$, $\langle r^2 \rangle$ and $\psi$ for both models were obtained using an optimization algorithm and discussed. It was found that the values of the transport radius $\langle r \rangle$ are in a good agreement with the mean radius obtained from the measurement of alumina texture.

**Key words**: Diffusion; Gas permeation; Porous structure model; Alumina; Porous materials.

Significant effort has been made to study of the dynamic multicomponent gas transport in porous materials, which have numerous applications in the industrial community. A proper description of transport processes such as diffusion or permeation combined with adsorption or chemical reaction is often necessary to choose, design and optimize the regime of adsorbers and chemical reactors.

One of the first pieces of information about dynamic transport of gases was published in the well-known book of Crank[1] in 1957. He introduced a system of partial differential equations (PDE's) and the diffusion was described by 2nd Fick's law for various geometric configurations of porous material (slab, cylinder or sphere). At present, the diffusion transport is often characterized by the modified Stefan–Maxwell constitutive equation and the permeation (gas transport forced by the pressure gradient) by the Darcy law, which are included in models of porous structure and comply with the reality more efficiently. In most published papers, a modified diffusion cell of the Wicke–Kallenbach type is employed for investigation of transient transport processes of inert gases (Novak *et al.*[2], Capek *et al.*[3,4], Tuchlenski *et al.*[5]).

The aim of this work was to compare transport parameters optimized on the basic assumptions of Mean Transport Pore Model[6] (MTPM) or Dusty Gas Model[7] (DGM) from the dynamic pressure responses to inert gas step changes in the Wicke–Kallenbach diffusion cell.

## THEORETICAL

### *Transport Models*

The two transport models, Mean Transport Pore Model (MTPM) and Dusty Gas Model (DGM), were used in this study to describe the porous structure of the bidispersed alumina. Both models are constituted on the basis of the kinetic theory of gases. In addition, the contribution of the bulk and Knudsen diffusion (transport parameters $\langle r\rangle\psi$, $\psi$), convectional viscous flow and Knudsen permeation ($\langle r^2\rangle\psi$, $\langle r\rangle\psi$) are the constituent parts of the considered models. The single constant $\langle r\rangle$ denotes a transport pore radius, $\langle r^2\rangle$ is the mean of the squared transport pore radii and $\psi$ means effective porosity. These constants only reflect the solid material properties and are not dependent on the intensive variables (pressure, temperature) and on the gases being transported in porous materials.

### *Diffusion and Permeation in Multicomponent Transport in Porous Material*

The key problem in the case of the multicomponent gas ($n$ components) transport in a porous material is the relation between net molar flux densities $\boldsymbol{N} = \{N_1, N_2,\ldots, N_n\}^{\mathrm{T}}$ and gradient of the molar concentrations $\boldsymbol{c} = \{c_1, c_2,\ldots, c_n\}^{\mathrm{T}}$, expressed in the condensed vector form as Eq. (*1*)

$$\boldsymbol{H}\cdot\boldsymbol{N} + \frac{\partial \boldsymbol{c}}{\partial x} = 0 \ , \qquad (1)$$

where $\boldsymbol{H}$ denotes the square matrix containing physicochemical properties of the transported gases (viscosities, molecular diffusion coefficients, Lennard–Jones potentials, *etc*.).

If multicomponent gas transport takes place by diffusion and permeation, then the net molar flux density for each gas component consists of partial molar flux densities $N_i^{\mathrm{dif}}$ and $N_i^{\mathrm{perm}}$, produced by both the mechanisms and Eq. (*2*) is valid

$$N_i = N_i^{\mathrm{dif}} + N_i^{\mathrm{perm}} \ . \qquad (2)$$

The inert component transported in pores by diffusion obeys under isothermal conditions the constitutive Maxwell–Stefan equation (*3*)

$$-c_{\mathrm{tot}}\frac{\mathrm{d}y_i}{\mathrm{d}x} = \frac{N_i^{\mathrm{dif}}}{D_i^{\mathrm{k}}} + \sum_{j=1,\, i\neq j}^{n}\frac{y_j N_i^{\mathrm{dif}} - y_i N_j^{\mathrm{dif}}}{D_{ij}^{\mathrm{m}}} \ , \qquad (3)$$

where $D_{ij}^{m}$ is the binary diffusion coefficient in the bulk region, $D_i^k$ is the diffusion coefficient in the Knudsen region, $c_{tot}$ represents total concentration and $y_i$ or $y_j$ are molar fractions of gases *i* and *j*, respectively. The Darcy equation (*4*) serves for complete description of the gas transport in pores, if a gradient of partial pressure exists (permeation mechanism)

$$N_i^{perm} = -B_i \frac{dp_i}{dx} \quad . \tag{4}$$

The permeability coefficient $B_i$ of *i*-th component depends on pressure; $p_i$ is its partial pressure.

*Mass Balance of the Modified Wicke–Kallenbach Cell*

Mass balance of the diffusion cell for a multicomponent gas mixture inside the porous material (*5*) supplements the constitutive Stefan–Maxwell equation (*1*)

$$-\frac{\partial \boldsymbol{N}}{\partial x} = \varepsilon \frac{\partial \boldsymbol{c}}{\partial t} \quad . \tag{5}$$

The boundary conditions (*6*) and (*7*) are derived from mass balance of the lower and upper compartments of the diffusion cell as

$$V_0 \frac{\partial \boldsymbol{c}}{\partial t} = -\frac{V_p}{L} \boldsymbol{N}(t,0) \tag{6}$$

$$V_L \frac{\partial \boldsymbol{c}}{\partial t} = F^0 \boldsymbol{c}^0 - F\boldsymbol{c} - \frac{V_p}{L} \boldsymbol{N}(t,L) \quad , \tag{7}$$

where $V_0$ and $V_L$ are the free volume of the lower and upper volume of the diffusion cell, respectively, and $V_p$ is the geometrical volume of the porous material, that is fixed by the cell holder. The upper compartment of the cell is flown by the gas (input/output volumetric flow $F^0/F$) and the lower one is closed. The whole system is entirely described by the initial conditions in Eq. (*8*) which characterize the state in the diffusion cell after flushing by the inert gas in time $t = 0$

$$\boldsymbol{c}(0,x) = \boldsymbol{c}^0 \quad . \tag{8}$$

They can be formulated as constant gas component concentrations $\boldsymbol{c}^0 = \{c_1^0, c_2^0, \ldots, c_n^0\}^T$ at the beginning of the dynamic experiment.

## EXPERIMENTAL

### Porous Material

The home-made porous material[8] on the basis of α-alumina (Pural SB, Condea Chemie, Germany) shaped as cylindrical pellets was used. The pellets were formed under pressure 58 MPa on a press machine. They were dried (2 days, 105 °C) and calcined (600 °C, 35 °C/h; cooling 10 h; 600 °C, 150 °C/h; 2 h constant temperature 1 200 °C; cooling).

The analysis of the prepared pellets was carried out on a helium pycnometer, mercury porosimeter and BET surface analyzer (all instruments Micromeritics, U.S.A.). The textural properties of the porous pellets are summarized in Table I. The porous pellets are bidispersed with mesopore and macropore maxima on the size distribution curve. The pressing pressure being very high suppressed the size of macropores in the pellets. It was found from the pore size distribution, that the mesopore representation is twice higher than the macropore representation.

### Wicke–Kallenbach Diffusion Cell

The scheme of the modified version of the Wicke–Kallenbach diffusion cell is shown in Fig. 1. The cell is divided by a perforated metal holder, carrying the porous material in the pellet form, into the upper and lower compartments. The upper compartment is constructed so that it works as a continuous stirred tank reactor (CSTR). The flow rate of the gas stream is regulated by mass-flowmeter controller (Theiva Co., Czech Republic). The four-way valve on the input of the upper cell compartment enables the switching of the gas streams. The lower compartment is closed. A sensitive pressure transducer (4-API-50, Jumo Wien GmbH., Austria) is mounted on the lower compartment bottom with a linear pressure range from –100 to +50 kPa. The dynamic pressure response of the cell to the step gas change is monitored and stored in standard PC.

### Experiments Under Dynamic Conditions

All experiments were performed in the diffusion cell at ambient laboratory conditions. Cylindrical pellets were forced into parallel holes of the metalic disc and sealed with silicone rubber. Thus, the circular pellet faces were opened to one-dimensional transport of gases. The upper compartment of the diffusion cell was flushed by an inert gas (*e.g.* nitrogen) until the pressure equilibrium among

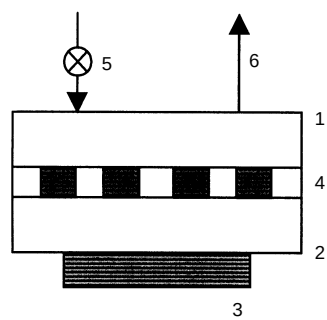


FIG. 1
Scheme of the Wicke–Kallenbach diffusion cell set-up. 1 Upper chamber of the cell, 2 lower chamber of the cell, 3 pressure transducer, 4 metallic disc with catalyst pellets, 5 gas input (gas step change), 6 gas output

both cell compartments (upper and lower) was established. The four-way valve was switched on at the beginning of the dynamic experiment and the first gas was replaced by the second (hydrogen). This step gas change is denoted as $N_2 \rightarrow H_2$. The pressure response of the diffusion cell reflects the transport processes (diffusion, permeation) in porous pellets. Hydrogen, helium, nitrogen and argon (standard purity grade 99.5% – Linde Co., Czech Republic) were used, to provide all dynamic runs.

Numerical Solution of the PDE's System and Transport Parameters Optimization

The PDE's system (*1*)–(*8*) was integrated by the method of lines[3]. Porous pellets were divided numerically into small volume elements to achieve discretization of the integral form (*5*). This numerical process produced the system of ordinary differential equations, which was solved by the backward differentiation formulas.

The three transport parameters, $\psi$, $\langle r \rangle$ and $\langle r^2 \rangle$, were obtained by minimization of the objective function $\chi^2$ defined as weighted sum of square deviations of calculated relative pressures $P^{\mathrm{calc}}(t)$ and experimentally determined relative pressures $P^{\mathrm{exp}}(t)$ in Eq. (*9*)

$$\chi^2 = \frac{1}{m} \sum_{i=1}^{m} \left[ P_i^{\mathrm{exp}}(t) - P_i^{\mathrm{calc}}(t) \right]^2 \quad . \tag{9}$$

The experimental pressure responses had different numbers $m$ of pairs $t$–$P(t)$ and therefore the weighted sum $\chi^2$ was chosen. The objective function (*9*) was minimized by the simplex algorithm of Nelder and Mead[9].

## RESULTS AND DISCUSSION

Experimental pressure responses were fitted using to the transport models MTPM and DGM. The values of the optimized transport parameters of both transport models are included in Table II. It can be confirmed from comparison of all three transport quantities that the transport parameters do not really depend on the kind of the transported

TABLE I
Geometric dimensions and textural properties of porous pellets

| Property | Value |
|---|---|
| Height/diameter, mm | 4.2/4.1 |
| Surface, $m^2\,g^{-1}$ | 6 |
| Porosity | 0.501 |
| Pore volume, $cm^3\,g^{-1}$ | 0.252 |
| Apparent density, g $cm^{-3}$ | 1.989 |
| True density, g $cm^{-3}$ | 3.986 |
| Mean mesopore radius, nm | 56 |
| Mean macropore radius, nm | 640 |

inert gas. The values of the calculated transport parameters $\psi$, $\langle r \rangle$ and $\langle r^2 \rangle$ for the single pressure responses induced by the step change of different gas combinations are quite similar.

Transport parameter $\psi$ equals $\varepsilon_t/q$, where $\varepsilon_t$ describes the porosity of transport pores and $q$ is tortuosity (lengthening of the real transport path relative to the ideal one). Thus this transport parameter characterizes the relative permeability of the porous material and can serve for comparison of transport properties of different porous materials. The values of $\psi$ obtained for both the considered transport models are comparable. The tortuosity is estimated as about 3 the value being considered in the literature satisfactory and real.

Consequently, the small difference between both models was investigated using the transport parameter $\langle r \rangle$ (see Table II). The transport pore radius $\langle r \rangle$ calculated for MTPM model falls in the region 500–600 nm. This fact corresponds to its value obtained experimentally from low-temperature adsorption of nitrogen (Table I, 640 nm). The optimized value of the transport radius $\langle r \rangle$ is somewhat lower because porous alumina has a small portion of mesopores and they can probably have a small effect on the binary gas transport.

The transport radius values $\langle r \rangle$ obtained for DGM are comparable with those from the MTPM model. The explanation may consist in the different conception of both the transport models. The MTPM model is based on the bundle of transport capillaries, whereas the DGM model is constructed on dust particles of porous material hold in their fixed positions by unspecified external forces[7]. Despite the fact that general theoretical background (kinetic theory of gases, Stefan–Maxwell constitutive equations) of both transport models is common, the MTPM model unlike DGM predicts different permeability coefficients $B_i$ for each component[3]. However, the calculated permeation molar flux densities could be somewhat different and, consequently, lead to different values of $\langle r \rangle$ for the DGM model.

TABLE II
Optimum MTPM and DGM transport parameters for the bidispersed alumina material

| Run | MTPM | | | | DGM | | | |
|---|---|---|---|---|---|---|---|---|
| | $\psi$ | $\langle r \rangle$, nm | $\langle r^2 \rangle$, nm$^2$ | $10^6\,\chi^2$ | $\psi$ | $\langle r \rangle$, nm | $\langle r^2 \rangle$, nm$^2$ | $10^6\,\chi^2$ |
| $H_2 \rightarrow N_2$ | 0.159 | 504 | 487 | 1.199 | 0.137 | 635 | 624 | 0.481 |
| $H_2 \rightarrow Ar$ | 0.149 | 505 | 587 | 6.062 | 0.114 | 678 | 607 | 1.957 |
| $He \rightarrow N_2$ | 0.124 | 616 | 498 | 2.615 | 0.129 | 654 | 732 | 1.496 |
| $He \rightarrow Ar$ | 0.136 | 534 | 586 | 3.383 | 0.110 | 683 | 699 | 1.790 |

The discrepancies in the values of the transport parameter $\langle r^2 \rangle$ reflect the above described situation for the transport pore radius $\langle r \rangle$. The interpretation of $\langle r^2 \rangle$ is based on the modified Hagen–Poisseille equation (*10*) for the permeation coefficient $B_i$

$$B_i = \frac{\langle r^2 \rangle \psi p}{8\mu} + D_i^k \frac{K_i + \omega}{K_i + 1} \quad , \tag{10}$$

where $D_i^k$ is the effective Knudsen diffusion coefficient, $K_i$ denotes Knudsen number and $\omega$ designs the slip by the pore wall. Because of the existence of wide pores, the second term in Eq. (*10*) is negligible and the gas transport takes place rather in the bulk region. This state is reflected in relatively high values of the $\langle r^2 \rangle$ for both transport models. In comparison with the industrial catalyst ICI 52/1, characterized by the same method[4], the transport processes in porous alumina, in particular permeation, predominate in the bulk region.

The objective function $\chi^2$ indicates a quality of the theoretical fit and is a little different for both the transport models. In DGM, this value is smaller than in the MTPM model (Table II). The Figs 2 and 3 illustrate this situation in a more suitable way.

## CONCLUSION

The method of transport parameter optimization of the experimental pressure responses from the Wicke–Kallenbach diffusion cell using the theoretical transport models

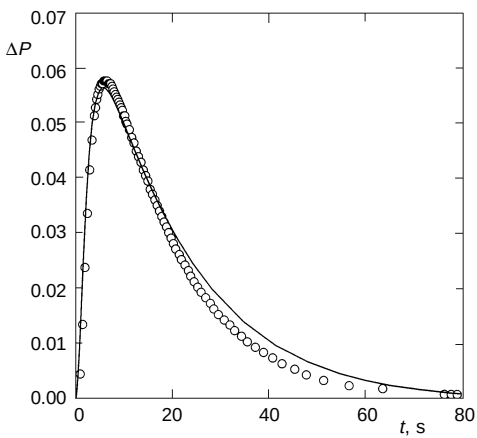


FIG. 2
The optimum MTPM fit of the pressure response of diffusion cell to the gas step change $H_2 \rightarrow Ar$; ❍ experiment, —— optimum MTPM fit

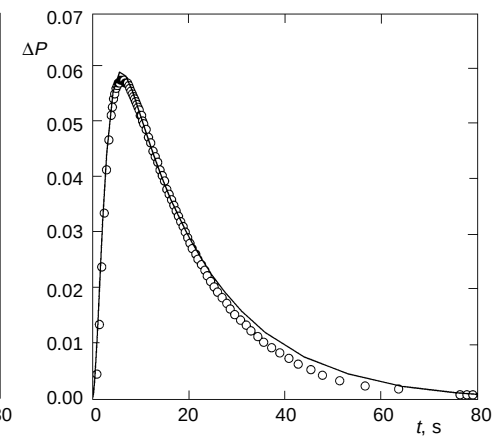


FIG. 3
The optimum DGM fit of the pressure response of diffusion cell to the gas step change $H_2 \rightarrow Ar$; ❍ experiment, —— optimum DGM fit

MTPM and DGM was applied to the binary gas transport in porous bidispersed alumina. The calculated results were found quite satisfied. The value of the transport radius $\langle r \rangle$ for the MTPM model is in an excellent agreement with the measurement using nitrogen adsorption. The differences between both transport models were explained on the basis of their own concepts and of different consideration of permeation mechanism. On the basis of comparison with similar experiments and calculations made for the industrial catalyst ICI 52/1, it can be claimed that this modern approach supplements the verified classical methods of the textural analysis.

## SYMBOLS

| | |
|---|---|
| $B$ | effective permeability of gas mixture (DGM), $cm^2\ s^{-1}$ |
| $B_i$ | effective permeability of $i$-th component (MTPM), $cm^2\ s^{-1}$ |
| $\boldsymbol{c}$ | vector of molar concentrations |
| $c_i$ | molar concentration of $i$-th component, mol $cm^{-3}$ |
| $c_{tot}$ | total molar concentration, mol $cm^{-3}$ |
| $D_{ij}^{m}$ | effective bulk diffusivity of components $i$, $j$, $cm^2\ s^{-1}$ |
| $D_i^{k}$ | effective Knudsen diffusivity of $i$-th component, $cm^2\ s^{-1}$ |
| $F^0$, $F$ | inlet or outlet flowrate of gas mixture, $cm^3\ s^{-1}$ |
| $\boldsymbol{H}$ | matrix of physicochemical properties of transported gases |
| $i$, $j$ | gas components |
| $K_i$ | Knudsen number of component $i$ |
| $L$ | pellet length, cm |
| $N_i$ | molar flux density of $i$-th component, mol $s^{-1}\ cm^{-2}$ |
| $\boldsymbol{N}$ | net molar flux density vector |
| $m$ | number of pairs in the pressure response |
| $n$ | number of gas components |
| $p$ | pressure, kPa |
| $P$ | relative pressure |
| $q$ | tortuosity |
| $\langle r \rangle$ | transport pore radius, nm |
| $\langle r^2 \rangle$ | mean squared transport pore radius, $nm^2$ |
| $R$ | universal gas constant, J $mol^{-1}\ K^{-1}$ |
| $t$ | time, s |
| $V$ | geometric volume, $cm^3$ |
| $y_i$ | molar fraction of $i$-th component |
| $x$ | length coordinate, cm |
| $\chi^2$ | objective function |
| $\varepsilon$ | pellet porosity |
| $\varepsilon_t$ | porosity of transport pores |
| $\lambda_i$ | mean free-path length of gas molecules $i$, cm |
| $\mu$ | gas mixture viscosity, Pas |
| $\psi$ | effective porosity |
| $\omega$ | slip coefficient |

Subscripts

| | |
|---|---|
| 0 | bottom part |

| | |
|---|---|
| L | top part |
| p | pellet |
| Superscripts | |
| 0 | initial |
| calc | calculated |
| dif | diffusional |
| exp | experimental |
| k | Knudsen |
| m | molecular |
| perm | permeation |
| T | transposed |

*This study was financially supported by the Grant Agency of the Academy of Sciences of the Czech Republic (project No. A4072706).*

## REFERENCES

1. Crank J.: *The Mathematics of Diffusion*, p. 121. Clarendon Press, Oxford 1957.
2. Novak M., Ehrhardt K., Klusacek K., Schneider P.: *Chem. Eng. Sci.* **1988**, *43*, 185.
3. Capek P., Hejtmanek V., Solcova O., Schneider P.: *Catal. Today* **1997**, *38*, 31.
4. Capek P., Hejtmanek V., Solcova O., Schneider P.: *Chem. Eng. J.*, in press.
5. Tuchlenski A., Schramm O., Seidel-Morgenstern A.: *Collect. Czech. Chem. Commun.* **1997**, *62*, 1043.
6. Schneider P.: *Chem. Eng. Sci.* **1978**, *33*, 1311.
7. Mason E. A., Malinauskas A. P.: *Gas Transport in Porous Media: The Dusty Gas Model*. Elsevier, Amsterdam 1983.
8. Valus J.: *Ph.D. Thesis.* Academy of Sciences of the Czech Republic, Prague 1983.
9. Himmelblau D. M.: *Nonlinear Programming*, p. 148. McGraw–Hill, New York 1972.